Heliyon xxx (xxxx) xxx

Contents lists available at ScienceDirect

Heliyon

journal homepage: www.cell.com/heliyon

Research article

Assessment of carboxyhemoglobin content in the blood with high accuracy: wavelength range optimization for nonlinear curve fitting of optical spectra

Elena Kozlova [a,b,*], Aleksandr Chernysh [a,b], Aleksandr Kozlov [b], Viktoria Sergunova [a], Ekaterina Sherstyukova [a,b]

[a] Federal Research and Clinical Center of Intensive Care Medicine and Rehabilitology, V.A. Negovsky Research Institute of General Reanimatology, 107031, 25 Petrovka Str., Build. 2, Moscow, Russian Federation

[b] Sechenov First Moscow State Medical University (Sechenov University), 119991, 2-4 Bolshaya Pirogovskaya St., Moscow, Russian Federation

ARTICLE INFO

Keywords:
Biophysics
Medical physics
Physics methods
Cell biology
Mathematical biosciences
Biochemistry
Hematological system
Toxicology
Intensive care
Carbon monoxide
Carboxyhemoglobin
Spectrophotometry
Nonlinear curve fitting
Intercolinearity of molar absorptivities
Absorption and scattering

ABSTRACT

The impact of carbon monoxide (CO) gas on the human organism is very dangerous. The affinity of CO to hemoglobin is considerably higher than that of oxygen. Thus, the interaction of CO with the blood results in a higher content of carboxyhemoglobin (*HbCO*) in red blood cells (RBCs) and correspondingly in tissue hypoxia. The disruption in the organism depends on the *HbCO* content in the blood. To assess any complications in the body at a given moment due to CO exposure and predict future consequences, it is necessary to measure the dynamics of hemoglobin derivative concentrations simultaneously. However, measuring *HbCO* and other derivatives in RBCs without hemolysis accurately is complicated due to the strong intercollinearity between the molar absorptivities of hemoglobin derivatives and superposition of absorption and scattering spectra. In the present study, to quantitatively assess the contents of the hemoglobin derivatives in the blood after exposure to CO, improved accuracy is achieved by optimizing the wavelength range used for the nonlinear curve fitting of optical spectra. Experimental spectra were measured in the wavelength range $\Delta\lambda = 500 - 700$ nm. For each experimental curve, it was established the value of optimal interval $\Delta\lambda_{opt}$ for which the correlation coefficient between experimental data and corresponding points of the theoretical fitting curve was the maximum in the wavelength range $\Delta\lambda_{typ} = 535 - 580\ nm$, which contains the typical absorption peaks for HbO_2, *Hb*, and *HbCO*. The concentrations obtained based on such fitting curves were considered to be highly accurate. The quantitative assessment enabled the determination of the *HbCO* nonlinear increase with the time of CO exposure in the *in vitro* experiment and the study of the dynamics of hemoglobin derivative transformations during blood incubation.

1. Introduction

The interaction of carbon monoxide (CO) with blood results in an increased amount of carboxyhemoglobin (*HbCO*). The affinity of CO to hemoglobin (Hb) is much higher (200–250 times) than that of oxygen (Bleecker, 2015; Gorman et al., 2003; Kinoshita et al., 2020; Oliverio; Varlet, 2018; Wu and Wang, 2005). Thus, CO exposure can cause tissue hypoxia. Due to the action of CO, free radicals may be generated, platelets may be activated, and the processes in mitochondria may be disrupted (Alonso et al., 2003; Kao and Nañagas, 2004; Oliverio; Varlet, 2018; Wu and Wang, 2005).

Some physiological processes are connected with endogenously produced CO (Gorman et al., 2003; Levitt; Levitt, 2015; Wu and Wang, 2005). However, exogenous intoxication plays the main role in these processes due to CO exposure (Bleecker, 2015; Kinoshita et al., 2020; Oliverio; Varlet, 2018; Wu and Wang, 2005).

The disruptions of the organism depend on the *HbCO* content in blood, which in turn depends on the intensity and duration of the CO action on biological objects (Kinoshita et al., 2020). In healthy blood, the concentration of *HbCO* is less than 1–2% (Kinoshita et al., 2020; Wu and Wang, 2005). For HbCO levels higher than 10%, neurological symptoms (dizziness, nausea, headache) can be observed (Kinoshita et al., 2020). At an *HbCO* level of 30–50%, a number of symptoms are observed such as syncope and increases in respiratory and heart rates (Kinoshita et al., 2020). *HbCO* concentrations greater than 50% are life-threatening (Kinoshita et al., 2020).

Elevated *HbCO* levels that are 7–14 times higher than those in normal blood may be found in packed red blood cells (RBCs) from donors who

* Corresponding author.
E-mail address: waterlake@mail.ru (E. Kozlova).

https://doi.org/10.1016/j.heliyon.2020.e04622
Received 8 March 2020; Received in revised form 9 June 2020; Accepted 30 July 2020

smoke (Boehm et al., 2019; Ehlers et al., 2003). At the same time, it is known that even at concentrations of 1–9%, *HbCO* may lead to chest pain and cause difficulties in exercising for some people with ischemic heart disease (Bleecker, 2015). Therefore, the *HbCO* level must be measured to improve the safety of packed RBC transfusion to patients, particularly to newborns and patients in critical condition (Boehm et al., 2019; Ehlers et al., 2003).

Thus, for the evaluation of clinical cases due to CO-poisoning in forensic medicine, it is very important to develop quantitative methods for the measurement of the *HbCO* level in the blood with high accuracy (Bleecker, 2015; Boumba and Vougiouklakis, 2005; Kao and Nañagas, 2004; Kinoshita et al., 2020). The most widely used methods for the determination of carboxyhemoglobin in whole blood are the spectrophotometric and the gas chromatographic methods (Boumba and Vougiouklakis, 2005).

The complications in the organism can appear at some point after its exposure to CO gas (Bleecker, 2015). Therefore, particularly for the task of assessing complications in the body at a given moment and predicting the future consequences of CO exposure, it is necessary to solve the problem of the dynamics of the mutual transformations of HbO_2 and *HbCO* to enable prediction of the time evolution of their concentrations. This problem is complicated by the possible rise in the content of other hemoglobin derivatives, in particular methemoglobin (*MetHb*), in the blood. Therefore, it is also necessary to improve the methods for the measurement of the hemoglobin derivative content to obtain high accuracy (Bickler and Rhodes, 2018). The content of *HbCO* in the blood can be measured by spectrophotometry (Boumba and Vougiouklakis, 2005; Kinoshita et al., 2020; Widdop, 2002). A number of spectrophotometry methods are based on measurements at few wavelengths (Hess, 2017; Lee et al., 2003; Widdop, 2002). A number of other methods analyze the data that can be obtained in a wide wavelength range. For these methods, it was suggested that the experimental data should be analyzed by spectral deconvolution using nonlinear curve fitting based on the Levenberg–Marquardt algorithm (Bellavia et al., 2013; Chernysh et al., 2018; Jensen, 2007; Kozlova et al., 2016, 2018).

In the development of spectrophotometric methods, it is necessary to consider the high degree of intercollinearity between the molar absorptivity coefficients of different hemoglobin derivatives. When assessing the content of *HBCO* in whole RBCs without hemolysis, the problem of intercollinearity is significantly compounded by the superposition of absorption and scattering spectra. In this case, an adequate evaluation of hemoglobin derivative content in the RBCs with high accuracy may be possible only by choosing the optimal spectral window for nonlinear curve fitting.

The purpose of this study is to optimize the wavelength interval for nonlinear curve fitting of optical spectra and to demonstrate the possibility of quantitative assessment of *HbCO* and other hemoglobin derivative content in RBCs with maximally high accuracy.

2. Materials and methods

2.1. Experimental scheme

The experimental stages (1–5) are schematically illustrated in Figure 1. All of the experiments were performed *in vitro*.

2.2. RBC suspensions for CO exposure and for spectrophotometry

In the experiments, we used blood provided by three women and three men. Experimental protocols were approved by the Federal Research and Clinical Center of Intensive Care Medicine and Rehabilitology, V.A. Negovsky Scientific Research Institute of General Reanimatology, Moscow, Russian Federation. Informed consent was obtained from all of the donors. Phosphate buffer (PBS) with pH 7.4 (200 µl, MP Biomedicals, France) was added to whole blood (150 µl) in microvettes with EDTA (Sarstedt AG & Co., Germany), as shown in Figure 1 (stage 1). The resulting hematocrit was 13–16%. This blood cell suspension was labeled *1*.

For spectrophotometry, blood cell suspension *1* (20 µl) was diluted in PBS 3 ml (blood cell suspension *2*), as shown in Figure 1 (stage 2).

2.3. Optical spectra registration by spectrophotometry

The measurement of the optical absorption spectra is the basis of the determination of the hemoglobin derivatives concentrations in RBC suspensions. A digital Unico 2800 spectrophotometer (United Products &

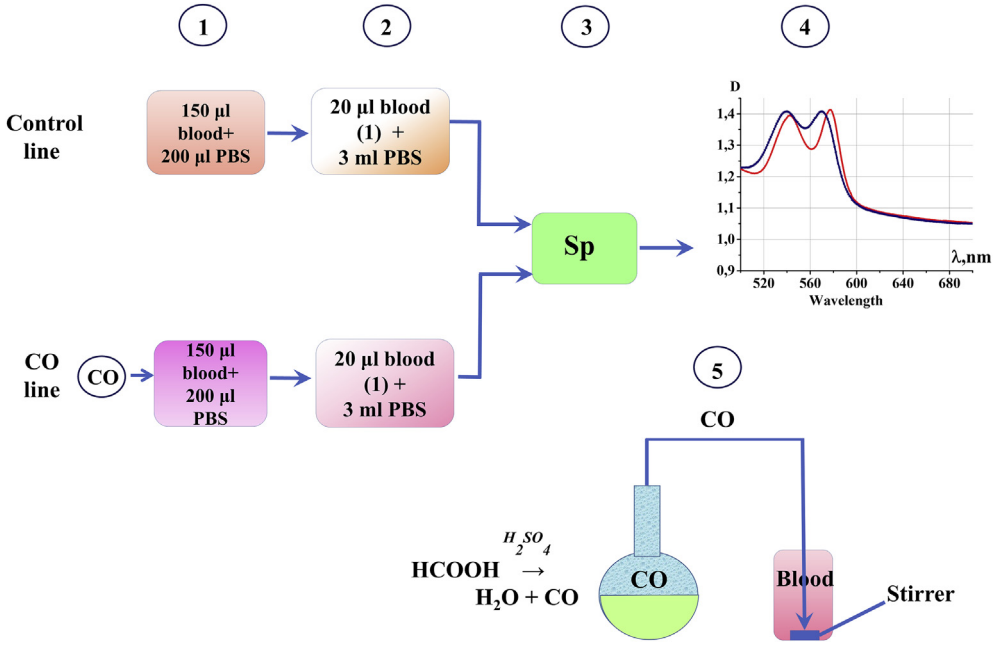

Figure 1. Experimental stages. 1 - preparation of the blood suspension for the control and CO exposure samples; 2 – the dilution of stage (1) suspension for the measurement of optical spectra; 3 - measurement of the absorption spectra by spectrophotometry; 4 – analysis of optical spectra; 5 – the system for the CO exposure in blood.

Instruments, USA) was used for the measurement of the absorbance spectra ($D_l(\lambda_l)_{exper}$) of the RBC suspension by standard methods (Bellavia et al., 2013; Chernysh et al., 2018; Kozlova et al., 2018) in the wavelength range $\Delta\lambda = 500 - 700\ nm$, with a step of 0.5–1 nm (Figure 1(3)).

Various hemoglobin derivatives have different typical absorption peaks at various wavelengths: the peaks for HbO_2 are located at 542 nm and 577 nm, the peak for deoxyhemoglobin (Hb) are located at 555 nm, the peak for *MetHb* is located at 630 nm, and the peaks for *HbCO* are located at 539 and 569 nm (Lu et al., 2015; Tift et al., 2014).

2.4. Nonlinear curve fitting for optical spectra

The aim of nonlinear fitting is to estimate the parameters that best describe the data (Figure 1 (stage 4)). For this purpose, it is necessary to experimentally obtain the set of optical densities measured at the corresponding wavelengths $D_l(\lambda_l)_{exper}$, where l is the wavelength index, and λ_l is the set of the measured wavelengths.

Then, we define our function $D_l(\lambda_l)_{theor}$ using Origin's flexible Fitting Function Builder in OriginPro (OriginLab Corporation, Northampton, MA, USA). This function is created according to biophysical considerations. Because the RBCs are studied in the PBS buffer, it is necessary to consider not only the absorption but also the scattering processes. The intensity of these processes will be different for various wavelengths. This approach was used successfully in our studies of the analysis of the absorption spectra after the influence of ultraviolet radiation (Kozlova et al., 2018) and $NaNO_2$ (Chernysh et al., 2018) on the blood. In the current experiments, *HbCO* is one of the main components. A total of four hemoglobin derivatives play important roles in the absorption process: HbO_2 , *Hb*, *MetHb* and *HbCO*. Thus, in the theoretical function a new term $\varepsilon_{HbCO,l}C_{HbCO}L$ is added to the equation of the optical density describing the absorption and scattering of light:

$$D_l(\lambda_l)_{theor} = \varepsilon_{HbO_{2,}\,l}C_{HbO_2}L + \varepsilon_{Hb,l}C_{Hb}L + \varepsilon_{MetHb,l}C_{MetHb}L + \varepsilon_{HbCO,l}C_{HbCO}L + K + \frac{S}{\lambda_l^4}. \quad (1)$$

In this equation, the known values are the molar absorptivity coefficients at the given wavelengths λ_l ($\varepsilon_{HbO_{2,}\,l}$, $\varepsilon_{Hb,l}$, $\varepsilon_{MetHb,l}$, and $\varepsilon_{HbCO,l}$) and the thickness of the layer L. The unknown values are the concentrations of the corresponding hemoglobin derivatives (C_{HbO_2}, C_{Hb}, C_{MetHb}, C_{HbCO}) and the scattering coefficients (K and S) . These parameters must be determined by model fitting. Coefficient K describes the scattering of light by RBC, when the wavelength is smaller than the RBC diameter d, $\lambda \ll d$. Coefficient S corresponds to Rayleigh scattering when the size of the scattering object d (roughness of the RBC membrane) is small, $\lambda \gg d$.

In the nonlinear curve fitting of the model, the experimental optical density data ($D_l(\lambda_l)_{exper}$) are used instead of $D_l(\lambda_l)_{theor}$. Computing the fitting values in a nonlinear regression is an iterative procedure performed by the Levenberg–Marquardt algorithm. The parameter values are adjusted iteratively to obtain the theoretical curve data closer to the experimental data. The obtained R-squared value provides a measure of the goodness of fit.

The total hemoglobin concentration $C(Hb_{tot})$ is the sum of the hemoglobin derivative concentrations, in *mmol/l*. The percentage of each derivative (content) in RBC is the ratio of its content to the total hemoglobin concentration; in particular, $C(HbCO) = 100\ \frac{C_{HbCO}}{C(Hb_{tot})}(\%)$.

2.5. Blood exposure to CO

Carbon monoxide (CO) was prepared by the standard method through the chemical reaction between formic acid and sulfuric acid (Bakovic et al., 2016; Yang et al., 2008):

$$HCOOH(formic\ acid) + H_2SO_4(sulfuric\ acid) \rightarrow CO + H_2SO_4 \cdot H_2O.$$

A scheme used to obtain bubbling of CO and evaluate its effects on blood cell suspension *1* is presented in Figure 1 (stage 5). For a one-time exposure (40 ± 10 s), 4 ml of formic acid (85%) was mixed with 4 ml of sulfuric acid (94%). A system consisting of a glass flask, where the chemical reactions were carried out to produce CO, and a gas-carrying glass tube was used (Figure 1 (stage 5)). The end of the tube was lowered into the microvette containing the blood at a distance of 2–4 mm from the bottom. Thus, CO bubbled through the entire blood suspension volume. Additionally, a magnetic stirrer was used to ensure the uniform exposure of the blood to the CO gas. Antiforming agent was not used when bubbling of CO to avoid additional effect on blood cells. After 40 ± 10 s of CO bubbling, intense foam developed in the glass flack. At this moment, the gas-carrying tube was pulled out, the used acids were poured out and fresh acids added into glass flack. Then the process of the formation of CO gas and its effect on blood cells was repeated. The total times of the blood cell suspension exposure to CO (t_{exp}) were t_{exp} = 80, 160, and 320 s.

After influence of CO gas on blood cell suspension *1*, this suspension was incubated at a temperature of 20–21 °C in room air. The time, during which the investigated blood cell suspension was kept under these specific conditions, is named incubation time t_{inc}. We measured optical spectra 1 h and 24 h after the exposure of the blood to CO (t_{inc} = 1 h and t_{inc} = 24 h). During 24 h of incubation the content of hemoglobin derivatives can be changed. Incubation time 24 h is often used as an upper limit for study of RBCs storaged without special conditions, for example as described in the work (Karsten et al., 2018).

2.6. Statistical analysis

OriginPro (OriginLab Corporation, Northampton, MA, USA) was used for descriptive statistics (correlation coefficients, data statistics), for nonlinear curve fitting analysis and for the calculation of correlation coefficients. As the control (not exposed to CO), the blood of six donors was used. The blood of four donors was exposed to CO. For each blood sample, the experiments were performed three times. Measured spectra and calculated concentrations of hemoglobin derivatives were obtained in each experiment. The figures show the mean values and standard deviations of the obtained data.

3. Results

Our results are presented according to this scheme:

1) the change in the absorption spectra due to the effect of CO on the blood;
2) selection of an optimal spectral window $\Delta\lambda_{opt}$ for obtaining adequate results for the hemoglobin derivative content, as shown in the example of control blood;
3) Quantitative assessment of the hemoglobin species content in the blood after the CO exposure in the model experiment. Identification of the quantitative pattern of the dynamics changes for the hemoglobin derivatives in the blood.

All experiments were performed *in vitro*.

3.1. Changes in the absorption spectra in the result of CO influence on blood

Representative obtained optical spectra for incubation time t_{inc} = 1 h are presented in Figure 2. These spectra correspond to the different times of the exposure of the blood to CO (t_{exp}). The percentages of the HbO_2, *Hb*, *MetHb*, and *HbCO* hemoglobin derivative contribute to the forms of the corresponding spectra observed for different exposure times. Light scattering also contributes to the observed spectra. This contribution can be observed in the base level of spectra (optical density is near 1.05).

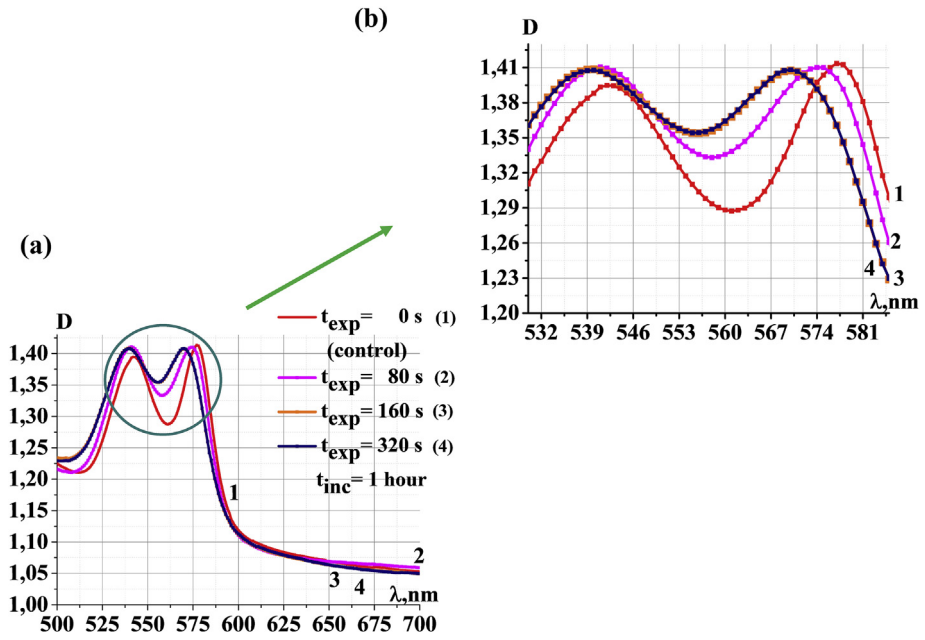

Figure 2. Optical spectra of the RBC suspensions: (a) Wavelength range $\Delta\lambda = 500 - 700$ *nm*; (b) Wavelength range $\Delta\lambda = 530 - 585$ *nm* (detailed image). 1 - t_{exp} = 0 s (control), 2 - t_{exp} = 80 s, 3 - t_{exp} = 160 s, 4 - t_{exp} = 320 s. Incubation timet_{inc} = 1 hour.

The peaks at the wavelength range $\Delta\lambda = 530 - 585$ *nm* are indicated by circles, and these detailed spectra are shown in Figure 2b.

During CO exposure, HbO_2 partially transformed to *HbCO*. Longer exposure time results in the shift of the optical density peaks to the left. Thus, for $t_{exp} = 0$ s (control blood), the peaks were located at 542 nm and 577 nm. For $t_{exp} = 80$ s, the peaks were observed at 541 nm and 574 nm. With increasing exposure time, the optical density peaks continued to shift and reached the maximum shift at λ = 540 nm and at λ = 570 nm for t_{exp} = 160 s. The same data were obtained for t_{exp} = 320 s. Thus, the saturation effect was observed.

3.2. Optimization of the wavelength range for the quantitative assessment of hemoglobin derivative content in blood

In the analysis of optical spectra of RBC suspension, it should be noted that molar absorptivities of hemoglobin derivatives are highly inter-

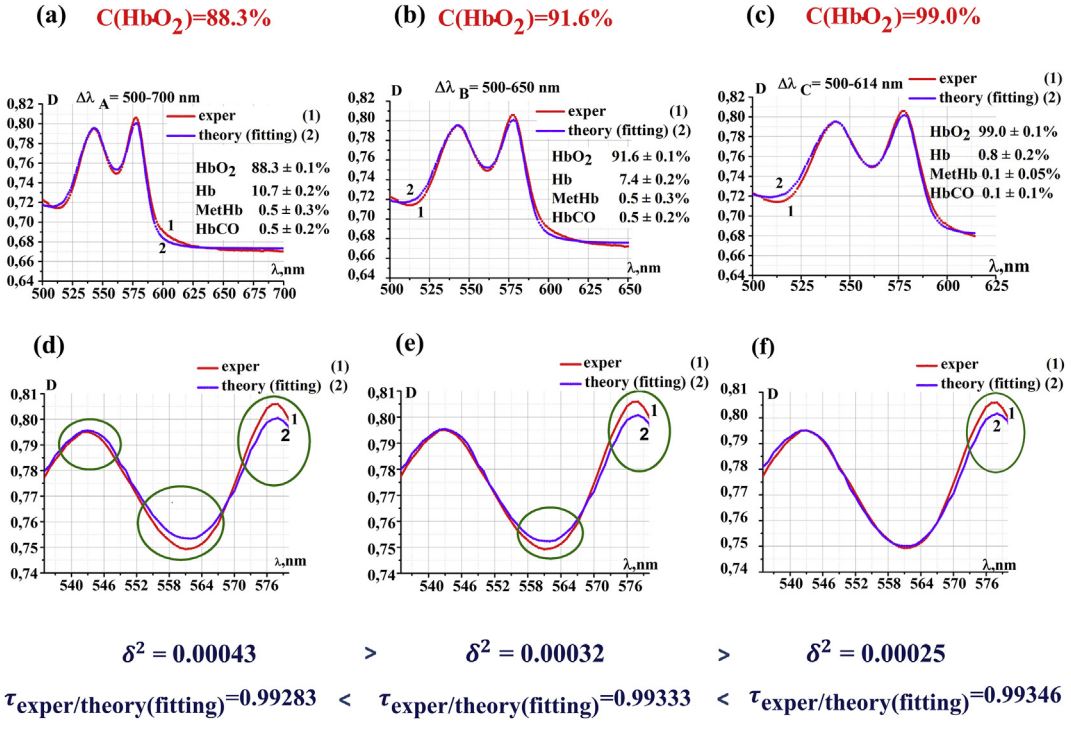

Figure 3. Choosing the wavelength interval for the accurate quantitative assessment of the content of hemoglobin derivatives in the blood by nonlinear curve fitting of optical spectra (control blood): (a) $\Delta\lambda_A$ = 500–700 nm; (b) $\Delta\lambda_B$ = 500–650 nm; (a) $\Delta\lambda_C$ = 500–614 nm; (d)–(f) detailed graphs at $\Delta\lambda_{typ} = 535 - 580$ *nm* corresponding to (a)–(c), the correlation coefficients $\tau_{exper/theor(fitting)}$ and the sum of squared deviations δ^2 are indicated for (d)–(f). 1- experimental data, 2 – fitting curve.

correlated: correlation coefficient between $\varepsilon_{HbO_2,\lambda}$ and $\varepsilon_{HbCO,\lambda}$ is $\tau = 0.95$, correlation coefficient between $\varepsilon_{Hb,\lambda}$ and $\varepsilon_{HbCO,\lambda}$ is $\tau = 0.94$), correlation coefficient between $\varepsilon_{HbO_2,\lambda}$ and $\varepsilon_{Hb,\lambda}$ is $\tau = 0.92$.

The concentrations C_{HbO_2}, C_{Hb}, C_{MetHb}, and C_{HbCO} are the unknown parameters. These concentrations were obtained by nonlinear curve fitting. We used the absorption and scattering model (Eq. 1) to fit the experimental spectra data. $D_l(\lambda_l)_{exper}$ was considered as the dependent variable. In the nonlinear curve fitting, the iterative adjusted of the parameter values obtained theoretical curves $D_l(\lambda_l)_{theor}$ that were close to the experimental data $D_l(\lambda_l)_{exper}$.

In contrast to our previous studies (Chernysh et al., 2018; Kozlova et al., 2016, 2018), in this study, we optimized the wavelength range to which the curve fitting was applied. This optimization was a necessary stage of quantitative analysis due to the high correlation of the molar coefficients of absorptivity for HbO_2, Hb and $HbCO$.

Figure 3 shows the results of the curve fitting and the quantitative assessment of the hemoglobin species content for control blood (without CO exposure) obtained in systematic experiments. In this case, we used the RBC suspension (5 μl whole blood in 3.4 ml PBS).

Fitting of the experimental data and the quantitative assessment of hemoglobin derivative concentrations were performed for 25–30 different wavelength ranges in the interval $\Delta\lambda = 500 - 700\ nm$, where the optical spectra were measured but none of the ranges was smaller than $\Delta\lambda_{min} = 530 - 590\ nm$. For each selected spectral window, the theoretical (fitting) curve was constructed according to Eq. (1) for the corresponding calculated parameters obtained by fitting. The correlation coefficient, $\tau_{exper/theor(fitting)}$, between the experimental data (1 in Figure 3) and the fitting curve (2 in Figure 3), was calculated in special typical interval $\Delta\lambda_{typ} = 535 - 580\ nm$. Additionally, the sum of squared deviations

$$\delta^2 = \sum_l \left(D_l(\lambda_l)_{exper} - D_l(\lambda_l)_{theor} \right)^2$$

in this typical interval $\Delta\lambda_{typ}$ was calculated. This interval $\Delta\lambda_{typ}$ corresponds to the typical absorption peaks of HbO_2, Hb, and $HbCO$ that are very close to each other.

The best curve was chosen from among the 25–30 obtained curves. The selection of the best curve was based on the fact that the correlation coefficient $\tau_{exper/theor(fitting)}$ is the maximum and, correspondingly δ^2 is the minimum, in the $\Delta\lambda_{typ}$ wavelength range. The concentrations of hemoglobin derivatives specified by this curve were considered correct.

As an example, Figure 3 shows three wavelength ranges chosen to fit the same experimental data: $\Delta\lambda_A = 500 - 700\ nm\ (a)$, $\Delta\lambda_B = 500 - 650\ nm\ (b)$, $\Delta\lambda_C = 500 - 614\ nm\ (c)$. In all of the graphs, the percentage of each hemoglobin derivative calculated using the spectral data in the corresponding interval is shown.

In the wavelength range (a), poor agreement is observed between the fitting curve data (2, blue) (taking into account the calculated concentrations in Eq. (1) obtained as a result of the fitting in this wavelength range) and the experimental data (1, red). Such poor matches of the data are indicated in the graphs by three green circles. For $\lambda = 554\ nm$, the theoretical values are higher, and for $\lambda = 577\ nm$, the theoretical values are lower than the experimental values (Figures 3 a,d). In the interval $\Delta\lambda_{typ}$, the correlation coefficient between $D_l(\lambda_l)_{theor}$ and $D_l(\lambda_l)_{exper}$ was $\tau_{exper/theor(fitting)} = 0.99283$. As a result, the calculated concentration of $C(HbO_2)$ was 88.3% ; this concentration was smaller than its true value (99–100%) that was obtained using a portable blood i-Stat®1 analyzer with the CG8+ cartridge (USA).

For wavelengths (b), the agreement was better (Figures 3b,e). Two green circles indicate the areas of poor agreement between the experimental and theoretical data. In this case, $\tau_{exper/theor(fitting)} = 0.99333$and $C(HbO_2) = 91.6\%$.

Finally, for wavelengths (c), only one green circle is observed in the figure. In this case, $\tau_{exper/theor(fitting)} = 0.99346$ and $C(HbO_2) = 99.0\%$.

In these three cases, the squares of the deviations δ^2 of the theoretical values from the corresponding experimental data in the range $\Delta\lambda_{typ}$ were calculated. It was found that $\delta_C^2 < \delta_B^2 < \delta_A^2$.

Thus, the interval $\Delta\lambda_C = 500$–614 nm was optimal $(\Delta\lambda_{opt})$ for fitting and calculation of the hemoglobin derivative concentrations. In this interval, the calculated content of HbO_2 was essentially in exact agreement with the value obtained by another standard method. Additionally, in this interval of fitting, the highest correlation coefficient $\tau_{exper/theor(fitting)}$ was obtained, and correspondingly, the δ^2 value was the smallest.

Thus, it was found that for the quantitative assessment of the hemoglobin derivative content in blood, it is necessary to choose the optimal interval $\Delta\lambda_{opt}$ for the fitting of the optical spectra. The optimality criterion is in the range of the typical absorption peaks $\Delta\lambda_{typ}$, the correlation coefficient between the theoretical and experimental data must be maximized, and correspondingly, the sum of squared deviations must be minimized. In this case, the calculated hemoglobin derivative concentrations can be considered to be true values.

3.3. Quantitative assessment of hemoglobin species content in the blood after CO exposure

3.3.1. Examples of using nonlinear curve fitting for the quantitative assessment of hemoglobin derivative concentrations for different CO exposure times

The concentrations and percentages of the hemoglobin derivatives in the blood before and after the action of the CO gas were calculated using the nonlinear curve fitting method and taking into account the need to choose the optimal wavelength range $\Delta\lambda_{opt}$. Figure 4 displays the experimental spectra data $D_l(\lambda_l)_{exper}$ and the theoretical fitting curves $D_l(\lambda_l)_{theor}$ that best describe the experimental data in the wavelength range $\Delta\lambda_{typ}$.

For all of the graphs, these intervals $\Delta\lambda_{opt}$ are indicated for each graph for different t_{exp} and t_{inc} (Figure 4). For the control data, $t_{exp} = 0$ s (Figure 4a) and for $t_{exp} = 80$ s, (Figure 4b), $\Delta\lambda_{opt} = 500 - 590\ nm$. For $t_{exp} = 320$ s and $t_{inc} = 1$ h, $\Delta\lambda_{opt} = 510 - 590\ nm$ (Figure 4c). For $t_{exp} = 320$ s and $t_{inc} = 24$ h, $\Delta\lambda_{opt} = 520 - 590\ nm$ (Figure 4d).

The calculated concentrations are shown in each graph (Figure 4). Figure 4a shows an example of the control data (without CO exposure). In this example, the main component was HbO_2, $C(HbO_2) = 95.8\%$.Figure 4b shows the experimental data and the theoretical curve for the optical densities obtained as a result of CO exposure for 80 s. In this case, $C(HbO_2) = 46.2\%$ and $C(HbCO) = 52.8\%$. Thus, the HbO_2 and $HbCO$ concentrations are almost the same. Figure 4c shows the results for the 320 s exposure of the blood to CO. The main component $HbCO$ reached $C(HbCO) = 87.9\%$. The experimental spectra in the cases described above were measured for one hour incubation after the CO exposure ($t_{inc} = 1$ h).

If the blood was incubated for 24 h after the CO exposure ($t_{exp} = 320$ s), changes in the hemoglobin derivative concentrations including $C(MetHb)$ were observed (Figure 4d).

3.3.2. Study of the dynamics of the hemoglobin derivative transformation in the result of CO exposure

The quantitative assessment of the hemoglobin derivative concentrations by the method described above enable the study of the dynamics of the transformation of the hemoglobin derivatives.

The concentration values varied with the time of blood exposure to CO (Figure 5a). A higher time of exposure (t_{exp}) corresponding to lower percentage of $HbO_2 + Hb$ and higher percentage of $HbCO$ was measured 1 h after the exposure of the blood to CO.

Meanwhile, the percentage of $MetHb$ remained unchanged$C(MetHb) = 0.5 \pm 0.5\%$. The graphs presented in Figure 5a show the obtained mean values and standard deviations of the hemoglobin derivative concentrations.

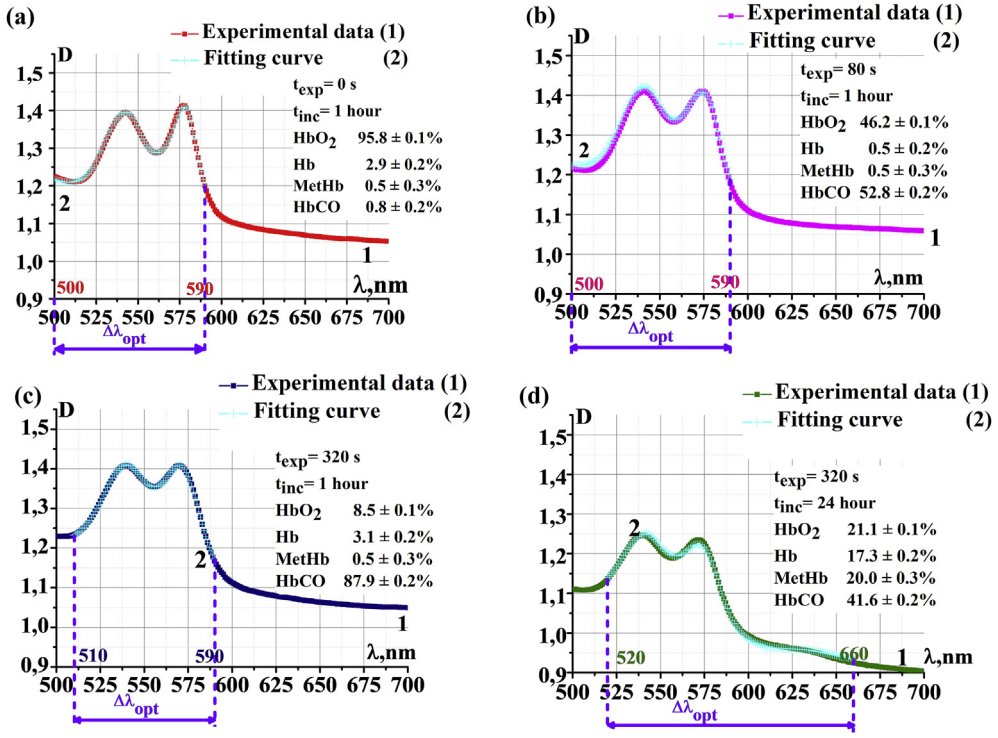

Figure 4. Wavelength intervals $\Delta\lambda_{opt}$ for the accurate quantitative assessment of the contents of the hemoglobin derivatives in the blood by the nonlinear curve fitting (2) of experimental optical spectra (1): (a) $\Delta\lambda_{opt} = 500 - 590$ *nm*, $t_{exp} = 0$ s (control), $t_{inc} = 1$ h, $C(HbCO) = 0.8\%$; (b) $\Delta\lambda_{opt} = 500 - 590$ *nm*, $t_{exp} = 80$ s, $t_{inc} = 1$ h, $C(HbCO) = 52.8\%$; (c) $\Delta\lambda_{opt} = 510 - 590$ *nm*, $t_{exp} = 320$ s, $t_{inc} = 1$ h, $C(HbCO) = 87.9\%$; (d) $\Delta\lambda_{opt} = 520 - 660$ *nm*, $t_{exp} = 320$ s, $t_{inc} = 24$ h, $C(HbCO) = 41.6\%$.

Photographs of the control suspension and RBC suspension after CO exposure during 320 s are shown in Figure 5 b. The control suspension was red (left) and assumed a pink-cherry color after CO exposure (right). The colors of the suspensions correspond to their percentages of different hemoglobin derivatives.

Incubation for 24 h after CO exposure led to a change in the ratios of the hemoglobin derivative percentage (Figure 6). The control data (without CO influence) are shown in Figures 6a,c. The percentages of hemoglobin derivatives in control blood after 1 h incubation and after 24 h of incubation were statistically the same. The hemoglobin derivatives were mainly HbO_2. Meanwhile, the *HbCO* content was no greater than 1%.

By contrast, the spectrum of the suspension, which was exposed to CO and then incubated for 24 h, was strongly different from the spectrum of

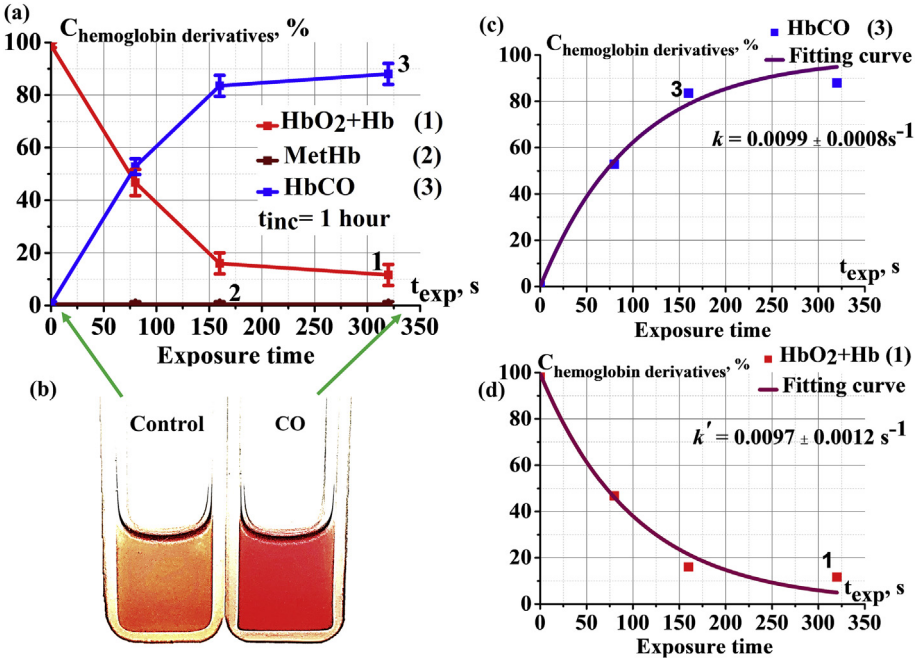

Figure 5. Dynamics of hemoglobin derivative transformation: (a) the change of $C(HbO_2) + C(Hb)$ (1), $C(MetHb)$ (2) , $C(HbCO)$ (3) for different CO exposure times t_{exp}; (b) photograph of RBC suspensions – control and after CO exposure; (c) experimental data for the increase of $C(HbCO)$ (3) with t_{exp} and the corresponding theoretical fitting curve; (d) experimental data for decreasing $C(HbO_2) + C(Hb)$(1) with t_{exp} and the corresponding theoretical fitting curve.

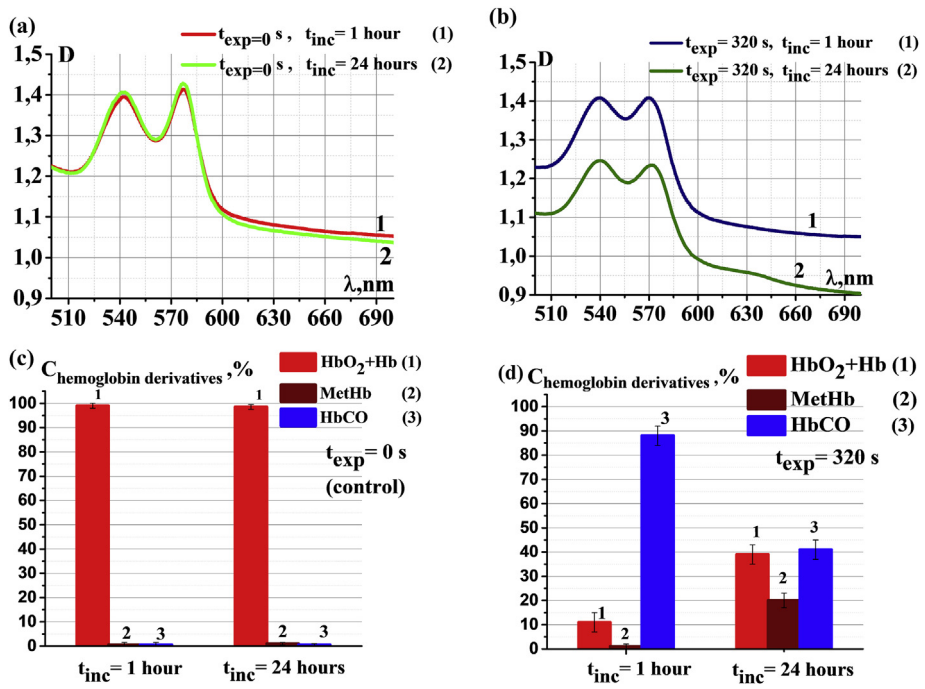

Figure 6. Experimental optical spectra and diagrams of the calculated concentrations of $C(HbO_2)+$ $C(Hb)$(1), $C(MetHb)$ (2), $C(HbCO)$ (3) for different incubation times t_{inc} = 1 h and t_{inc} = 24 h: (a), (d) t_{exp} = 0 s (control); (b), (d) for t_{exp} = 320 s.

the suspension with the incubation time of 1 h (Figure 6b). A change in the spectrum indicates a change in the contents of the hemoglobin derivatives in the suspension. In addition, in this case, the percentage of *HbCO* decreased strongly from $C(HbCO) = 88 \pm 5\%$ to $C(HbCO) = 41 \pm 4\%$. In turn, $C(HbO_2 + Hb)$ increased from $C(HbO_2 + Hb) = 12 \pm 3\%$ to $C(HbO_2 + Hb) = 39 \pm 4\%$. Interestingly, *MetHb* concentration increased significantly from $C(MetHb) = 0.5 \pm 0.5\%$ to $C(MetHb) = 20 \pm 3\%$. These results obtained *in vitro* are important for blood analyze after body intoxication by CO *in vivo*, because *MetHb* as well as *HbCO* cannot deliver oxygen to tissues.

It should be noted that a decrease in the level in the spectrum from 1.1 to 0.9 was observed (Figure 6d).

4. Discussion

In this work, for quantitative processing of optical spectra, we used the nonlinear curve fitting method. When quantifying the hemoglobin derivative concentrations in the blood, the difficulties associated with the strong correlations between their molar absorption coefficients $\varepsilon_{HbO_2,\lambda}$, $\varepsilon_{Hb,\lambda}$, and $\varepsilon_{HbCO,\lambda}$ (the correlation coefficient $\tau > 0.92$) must be addressed. In a number of studies, the nonlinear curve fitting method was proposed. As a rule, hemoglobin absorption spectra in hemolyzed solutions are used for analysis (Bellavia et al., 2013; Jensen, 2007; Kozlova et al., 2016).

In this work, we use nonlinear curve fitting to analyze the absorption spectra of a suspension of the whole RBCs in a buffer. Here, we take into account not only the absorption but also the scattering of light at RBSs without the need for cell hemolysis (Chernysh et al., 2018). This consideration allows us to maintain the natural state of the hemoglobin inside the RBC during the measurement. Thus, we can analyze the hemoglobin derivatives both in and out of RBCs.

To accurately estimate the concentrations of hemoglobin derivatives, optimization of the wavelength interval $\Delta\lambda_{opt}$ used for the nonlinear curve fitting was performed (Figures 3 and 4). This interval is chosen so as to maximize the correlation coefficient between the theoretical and experimental data, and accordingly, the sum of the deviation squares is minimized in the interval $\Delta\lambda_{typ}$. The typical peak wavelengths of the hemoglobin derivatives investigated in this study are found in this wavelength range $\Delta\lambda_{typ}$. In this case, the theoretical fitting curve $D_l(\lambda_l)_{theor}$ best describes the experimental data $D_l(\lambda_l)_{exper}$, and a quantitative estimation of the concentrations (Figures 3 and 4) will be highly accurate.

Eq. (1) of the theoretical curve includes not only the concentrations of hemoglobin derivatives but also the scattering coefficients K and S. Therefore, changes in their values during blood storage after the exposure to an external factor can be used to estimate the percentage of hemolyzed erythrocytes. This estimate is important when discussing the mechanisms of the CO effect on the blood cells.

Experimentally, we found that the level of *HbCO* increases with the time of the blood exposure to CO. Moreover, the time dependence of *HbCO* concentration, $C(HbCO) = f(t_{exp})$, is nonlinear. Based on the experimental data, it was established that the dependence has the following form:

$$C(HbCO) = C(HbCO)_0 + \left(C(HbO_2)_0 + C(Hb)_0\right)\left(1 - e^{-kt_{exp}}\right), \quad (2)$$

where the subscript zero in this equation means $t_{exp} = 0$, and all concentrations are in %.

Time t_{exp} determines the dose of CO affecting the blood. Thus, we can consider Eq. (2) as being dose-dependent. In this case, the dose is given by $D = Flow\,(CO) \cdot t_{exp}$.

The coefficient k, which is the *HbCO* formation constant, was estimated from the experimental data (Figure 5a, c (3)).

An increase in the *HbCO* content is accompanied by a corresponding decrease in the concentration of oxy- and deoxyhemoglobin (Figure 5. (1)). The dose dependence of the decrease in their content is described by:

$$C(HbO_2) + CHb)\big) = C(HbO_2)_0 + C(Hb)_0\big)\, e^{-k' t_{exp}}, \quad (3)$$

where the coefficient k', which is the constant of the decrease in the oxy- and deoxyhemoglobin concentrations, can also be estimated from the experimental data. Using nonlinear curve fitting for the data (1, 3) in Figures 5c,d, we obtain:

$k = 0.0099 \pm 0.0008\ s^{-1}$ and $k' = 0.0097 \pm 0.0012\ s^{-1}$.

This outcome directly indicates that, in the process of CO exposure, oxyhemoglobin and deoxyhemoglobin are involved in the appearance of *HbCO*. In addition, methemoglobin does not participate in this transformation. The effect of the saturation of the *HbCO* concentration is associated with a gradual decrease in the concentration of HbO_2 and *Hb* in the suspension to small values during the transformation. Nonlinear dependence can be considered to predict the formation of *HbCO* in the body after exposure to CO. In the development of biomarkers [5], it is also important to assess the dose of CO exposure of the body.

After 24 h incubation of CO-exposed RBCs, a partial conversion of *HbCO* to oxyhemoglobin and deoxyhemoglobin was observed. Under the conditions of this experiment, approximately half of the *HbCO* participated in this transformation. After 24 h incubation of CO-exposed RBCs, a decrease in the level was observed in the spectrum (Figure 6b). This decrease indicates the partial hemolysis of RBCs in the blood. The formation of methemoglobin in the suspension may be associated with this partial hemolysis because free hemoglobin is easily oxidized into methemoglobin. This association can be considered in the *in vitro* experiments in the analysis of the clinical effects of the CO on the human organism.

The approach of choosing the optimal spectral interval $\Delta\lambda_{opt}$ in the analysis of the optical spectra by nonlinear curve fitting can be useful not only for the analysis of the content of hemoglobin derivatives in the blood but also for various other substances in different mixtures.

5. Conclusion

The nonlinear curve fitting method can be used efficiently to quantify the concentrations of *HbCO* and simultaneously of other hemoglobin derivatives in the blood only on the basis of the optical spectrum of the RBC suspension, without the use of any additional chemicals. It is shown that for an accurate quantitative assessment of the hemoglobin derivative concentrations, in particular of *HbCO*, it is necessary to choose the wavelength range $\Delta\lambda_{opt}$ for which the theoretical data best describe the experimental data. These results can be useful in the study of biophysical and biochemical processes in the blood after carbon monoxide exposure and for the analysis of the clinical implications of CO exposure of the organism.

Declarations

Author contribution statement

E. Kozlova and A. Kozlov: Conceived and designed the experiments; Performed the experiments; Analyzed and interpreted the data; Wrote the paper.

A. Chernysh: Conceived and designed the experiments; Analyzed and interpreted the data; Wrote the paper.

V. Sergunova: Conceived and designed the experiments; Performed the experiments; Analyzed and interpreted the data; Contributed reagents, materials, analysis tools or data; Wrote the paper.

E. Sherstyukova: Performed the experiments; Analyzed and interpreted the data; Contributed reagents, materials, analysis tools or data; Wrote the paper.

Funding statement

This work was supported by the Ministry of Science and Higher Education of the Russian Federation, Contract N 075-01414-20-02, Russian Academic Excellence Project 5-100.

Competing interest statement

The authors declare no conflict of interest.

Additional information

No additional information is available for this paper.

Acknowledgements

The authors would like to thank Elsevier Language Editing Services for English language editing.

The authors thank Olga Gudkova for the help with calculations.

References

Alonso, J.R., Cardellach, F., López, S., Casademont, J., Miró, Ò., 2003. Carbon monoxide specifically inhibits cytochrome c oxidase of human mitochondrial respiratory chain. Pharmacol. Toxicol. 93 (3), 142–146.

Bakovic, M., Nestic, M., Mayer, D., 2016. Suicidal chemistry: combined intoxication with carbon monoxide and formic acid. Int. J. Legal Med. 130 (3), 723–729.

Bellavia, L., DuMond, J.F., Perlegas, A., King, S.B., Kim-Shapiro, D.B., 2013. Nitroxyl accelerates the oxidation of oxyhemoglobin by nitrite. Nitric Oxide 31, 38–47.

Bickler, M.P., Rhodes, L.J., 2018. Accuracy of detection of carboxyhemoglobin and methemoglobin in human and bovine blood with an inexpensive, pocket-size infrared scanner. PloS One 13 (3), e0193891. . Published online 2018 Mar 7.

Bleecker, M.L., 2015. Carbon monoxide intoxication. Handb. Clin. Neurol. 131, 191–203.

Boehm, R., Cohen, C., Pulcinelli, R., Caletti, G., Balsan, A., Nascimento, S., Rocha, R., Calderon, E., Saint′Pierre, T., Garcia, S., Sekine, L., Onsten, Y., Gioda, A., Gomez, R., 2019. Toxic elements in packed red blood cells from smoker donors: a risk for paediatric transfusion? Vox Sang. 114 (8), 808–815.

Boumba, V.A., Vougiouklakis, T., 2005. Evaluation of the methods used for carboxyhemoglobin analysis in postmortem blood. Int. J. Toxicol. 24 (4), 275–281.

Chernysh, A.M., Kozlova, E.K., Moroz, V.V., Sergunova, V.A., Gudkova, O.E., Manchenko, E.A., Kozlov, A.P., 2018. Effects of succinate-based antioxidant on in vitro conversion of methemoglobin in oxyhemoglobin. Obshchaya Reanimatologiya= General Reanimatology 14 (2), 46–59.

Ehlers, M., McCloskey, D., Devejian, N.S., 2003. Alarming levels of carboxyhemoglobin in a unit of banked blood. Anesth. Analg. 97 (1), 289–290.

Gorman, D., Drewry, A., Huang, Y.L., Sames, C., 2003. The clinical toxicology of carbon monoxide. Toxicology 187 (1), 25–38.

Hess, D.R., 2017. Inhaled carbon monoxide: from toxin to therapy. Respir. Care 62 (10), 1333–1342.

Jensen, F.B., 2007. Nitric oxide formation from nitrite in zebrafish. J. Exp. Biol. 210 (19), 3387–3394.

Kao, L.W., Nañagas, K.A., 2004. Carbon monoxide poisoning. Emerg. Med. Clin. 22 (4), 985–1018.

Karsten, E., Breen, E., Herbert, B.R., 2018. Red blood cells are dynamic reservoirs of cytokines. Sci. Rep. 8, 3101.

Kinoshita, H., Türkan, H., Vucinic, S., Naqvi, S., Bedair, R., Rezaee, R., Tsatsakis, A., 2020. Carbon monoxide poisoning. Toxicol. Rep. 7, 169–173.

Kozlova, E., Chernysh, A., Sergunova, V., Gudkova, O., Manchenko, E., Kozlov, A., 2018. Atomic force microscopy study of red blood cell membrane nanostructure during oxidation-reduction processes. J. Mol. Recogn. 31 (10), e2724.

Kozlova, E., Chernysh, A., Moroz, V., Sergunova, V., Zavialova, A., Kuzovlev, A., 2016. Nanoparticles of perfluorocarbon emulsion contribute to the reduction of methemoglobin to oxyhemoglobin. Int. J. Pharm. 497 (1-2), 88–95.

Lee, C.W., Tam, J.C., Kung, L.K., Yim, L.K., 2003. Validity of CO-oximetric determination of carboxyhaemoglobin in putrefying blood and body cavity fluid. Forensic Sci. Int. 132 (2), 153–156.

Levitt, D.G., Levitt, M.D., 2015. Carbon monoxide: a critical quantitative analysis and review of the extent and limitations of its second messenger function. Clin. Pharmacol. 7, 37.

Lu, G., Qin, X., Wang, D., Chen, Z.G., Fei, B., 2015. Estimation of tissue optical parameters with hyperspectral imaging and spectral unmixing. Proc. SPIE-Int. Soc. Opt. Eng. 9417, 94170Q.

Oliverio, S., Varlet, V., 2018. Carbon monoxide analysis method in human blood by airtight gas syringe–gas chromatography–mass spectrometry (AGS-GC-MS): relevance for postmortem poisoning diagnosis. J. Chromatogr. B Analyt. Technol. Biomed. Life Sci. 1090, 81–89.

Tift, M.S., Ponganis, P.J., Crocker, D.E., 2014. Elevated carboxyhemoglobin in a marine mammal, the northern elephant seal. J. Exp. Biol. 217 (10), 1752–1757.

Widdop, B., 2002. Analysis of carbon monoxide. Ann. Clin. Biochem. 39 (4), 378–391.

Wu, L., Wang, R., 2005. Carbon monoxide: endogenous production, physiological functions, and pharmacological applications. Pharmacol. Rev. 57 (4), 585–630.

Yang, C.C., Ger, J., Li, C.F., 2008. Formic acid: a rare but deadly source of carbon monoxide poisoning. Clin. Toxicol. (Phila). 46 (4), 287–289.